The effects of feeding on cell morphology and proliferation of the gastrointestinal tract of juvenile Burmese pythons (*Python molurus*)

Cécile Helmstetter, Robert K. Pope, Mathieu T'Flachebba, Stephen M. Secor, and Jean-Hervé Lignot

Abstract: The gastrointestinal tract of Burmese pythons (*Python molurus* (L., 1758)) exhibits large morphological and physiological changes in response to feeding and extended periods of fasting. In this study the mucosa of the stomach, small intestine, and colon were examined for changes in structure and cellular proliferation. The mucosa of fasting pythons exhibited low levels of cellular replication, but after feeding, cellular replication was evident as early as 12 h in the small intestine and colon and 24 h in the stomach. Replication peaked 3 days postfeeding for the small intestine and colon, but was still increasing at 6 days postfeeding in the stomach. Interestingly, cell proliferation was still evident after 45 days in the colon. In these tissues, a stock of "ready-to-use" primary lysosomes is found in the mucosal cells of fasting animals, whereas profound intracellular recycling is typical of animals that have been fed. These findings indicate that during the postprandial period, the intestinal mucosa undergoes extensive remodelling in anticipation of the next fasting and feeding period. One key adaptive factor for the python's ability to cope with infrequent feeding is a well-prepared digestive system in fasting animals that can quickly start functioning again when food becomes available.

Résumé : Le tractus gastro-intestinal du python de Birmanie (*Python molurus* (L., 1758)) subit d'importants changements morphologiques et physiologiques en réaction à des nourrissages suivis de longues périodes de jeûne. Nous avons examiné les changements de structure et de prolifération cellulaire dans les parois muqueuses de l'estomac, de l'intestin grêle et du colon. Chez les pythons à jeun, tous les organes étudiés ont présentés un très faible niveau de prolifération cellulaire. Cependant, la production de nouvelles cellules a été observée dès 12 h après la réalimentation dans l'intestin grêle et le colon et après 24 h dans l'estomac. Cette prolifération atteint un maximum 3 jours après la réalimentation dans l'intestin grêle et le colon, mais elle augmente toujours dans l'estomac après 6 jours. Curieusement, la prolifération reste toujours détectable dans le colon malgré un jeûne de 45 jours. Dans toutes les cellules épithéliales, un large réservoir de lysosomes primaires « prêts à l'emploi » se retrouve chez les animaux à jeun, tandis qu'un profond recyclage intracellulaire se produit chez les animaux nourris. Ainsi, pendant la période postprandiale, la muqueuse digestive se modifie profondément et anticipe la prochaine période de jeûne et de réalimentation. Un des facteurs adaptatifs clés expliquant la capacité des pythons molures de résister à des réalimentations imprévisibles consiste ainsi à posséder chez les animaux à jeun un système digestif bien préparé et qui peut très rapidement se remettre en fonctionnement lorsque la nourriture est de nouveau disponible.

Introduction

With feeding, the Burmese python (*Python molurus* (L., 1758)) experiences a rapid upregulation of performance of the gastrointestinal tract (Secor and Diamond 1995). Within 24 h postfeeding (HPF), gastric luminal acidity drops from near neutral pH values to pH values as low as 2. This is accompanied by the release of pepsinogen, which is rapidly activated to the protease pepsin (Cox and Secor 2008). Peaks in intestinal form and function occur after 2 or 3 days of digestion, leading to a combined 10- to 25-fold increase in intestinal mass and mass-specific rates (Secor and Diamond 1995, 1997; Cox and Secor 2008). Within 1 day postfeeding (DPF), the small intestine increases in mass by 70%, the microvilli have quadrupled in length, and intestinal nutrient uptake rates and enzyme activities rise from 3- to 10-fold (Secor and Diamond 1995; Lignot et al. 2005; Cox and Secor 2008). When the last of the meal exits the stomach and passes into the small intestine, the gastrointestinal tract begins downregulating its structure and function; gastric acid secretion ceases, the intestine begins to atrophy, microvilli shorten, and intestinal nutrient transporter and enzyme activities are severely reduced (Secor and Diamond 1995; Lignot et al. 2005; Cox and Secor 2008). The two main postprandial responses observed within the python intestine, namely the increase in mass and the upregulation of nutrient uptake and enzyme activity, are characteristic of many animals following an episode of fasting, though to a lesser extent (Altmann 1972; Buts et al. 1990; Yamauchi et al. 1996; Waheed and Gupta 1997; Dou et al. 2001; Dunel-Erb et al. 2001). The repeated doubling of intestinal mass with each meal as experienced by Burmese pythons is an exceptional response, with the exception, however, of

Received 26 May 2009. Accepted 9 September 2009. Published on the NRC Research Press Web site at cjz.nrc.ca on 4 December 2009.

C. Helmstetter, R.K. Pope, M. T'Flachebba, and J.-H. Lignot.[1] Centre National de la Recherche Scientifique, Centre d'Ecologie et Physiologie Energétiques, 23 rue Becquerel, F-67087 Strasbourg CEDEX 2, France.
S.M. Secor. Department of Biological Sciences, Box 870344, The University of Alabama, Tuscaloosa, AL 35487-0344, USA.

[1]Corresponding author (e-mail: J-H.Lignot@c-strasbourg.fr).

Fig. 1. View of dissected Burmese pythons (*Python molurus*) at different time points after feeding. (A) Fasted. (B) 12 h postfeeding (HPF). Note the diameter of the intestine that enlarges considerably and fat bodies that are more numerous after feeding compared with the fasting status. (C) Digestive tract extracted from the body and with the mesenteric plexus taken out. Note the position of the gallblader and pancreas immediately below the thick pyloric sphincter and the presence of a large caecum. (D, E, F, G) Stomach cut open longitudinally: fasted snake, after 12 HPF, 3 days post feeding (DPF), and 6 DPF, respectively. Note that the digestion of the prey within the fundic region occurs within hours after ingestion. Ca, caecum; Car, cardiac region of the stomach; Co, colon; FB, Fat Bodies; Fund, fundic region; GB, gall bladder; Int: intestine; P, pancreas; Pr, prey; Pyl, pyloric region; PS, pyloric sphincter. Scale bars = 5 cm.

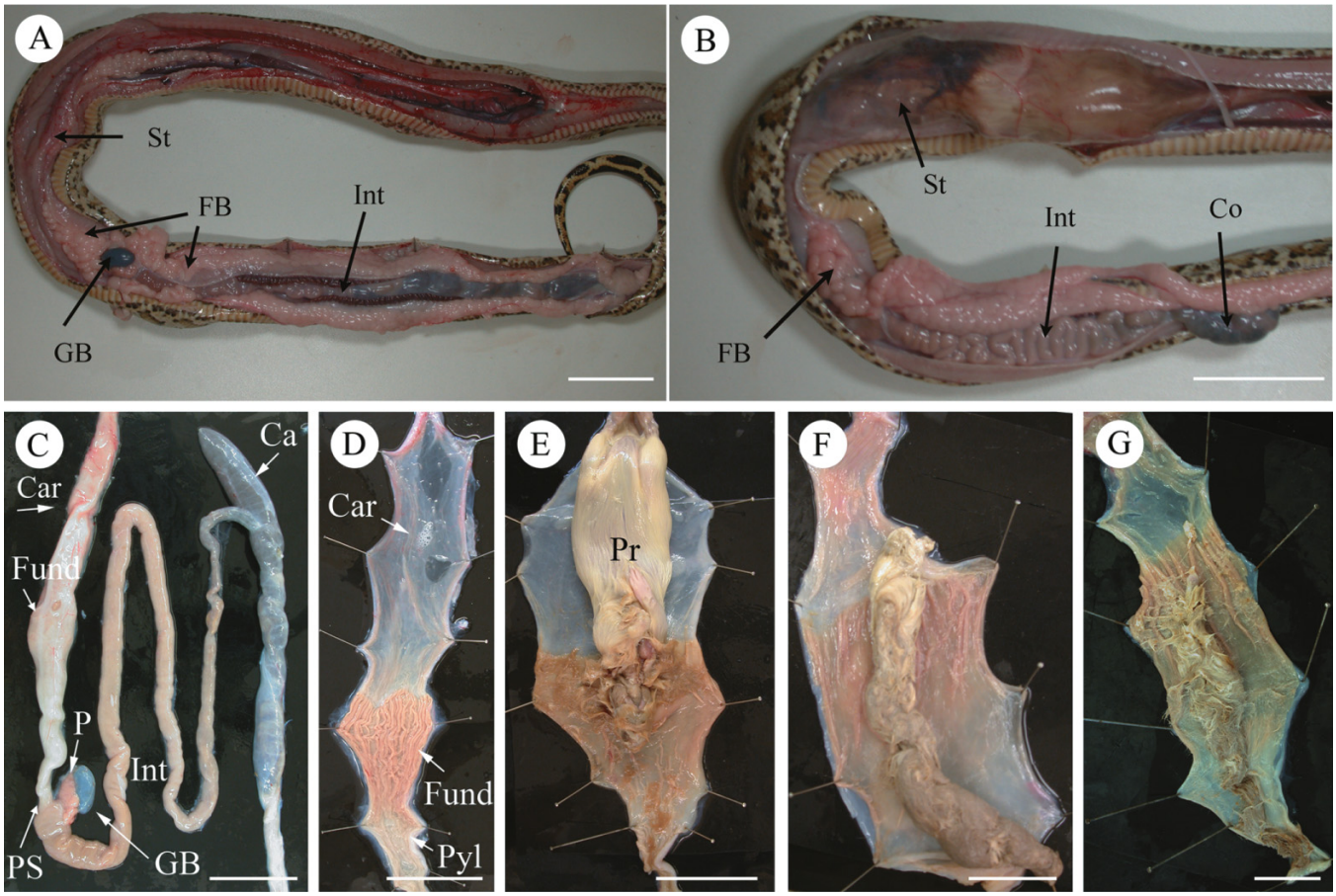

ground squirrels following hibernation and active anurans after estivation (each increasing small-intestinal mass by 2- to 3-fold) (Carey 1990; Secor and Diamond 1995, 1997; Starck and Beese 2001).

There are two potential mechanisms responsible for the growth of the python's gastrointestinal lining: cell hypertrophy and cell hyperplasia. Hypertrophy, which is growth via an increase in cell size, has been identified to be instrumental in the postprandial growth of the python's intestinal mucosa (Lignot et al. 2005). Intestinal enterocytes of Burmese pythons increase in width by 30% within 6 DPF. This growth can be partly explained by the absorption of luminal amino acids and lipids originating from the meal. This is most evident for enterocytes along the tips and edges of villi, many of which possess lipid droplets for several days after feeding (Starck and Beese 2001; Lignot et al. 2005). However, intestinal hyperplasia, which is growth via an increase in the number of cells, also occurs in fed Burmese pythons (Starck and Beese 2001). Cell proliferation increases from 1.67% in fasted animals up to 3.7% in 10 DPF. However, this is counterbalanced by an increase in programmed cell death (apoptosis), which also occurs during the postprandial period at a higher rate than in fasting snakes (Starck and Beese 2001). This indicates that a significant portion of the mucosal cells are replaced during the postprandial period, whereas the nonreplicating cells must respond morphologically to fasting and refeeding. Therefore, a more comprehensive study on these mechanisms is required to understand how mucosal cells can withstand repeated cycles of fasting and refeeding. Also tested is how cell proliferation is regulated along the digestive tract according to the timing for prey digestion in the stomach and nutrient assimilation in the small and large intestines. A final hypothesis is that hypertrophy for the large intestine may peak later than those for the stomach and small intestine.

Materials and methods

Animals and dissection

Hatchling Burmese pythons (~100 g) were purchased from commercial breeders (Zooland, Strasbourg, France) and maintained individually in a temperature-controlled room (28–30 °C) under a 14 h light : 10 h dark cycle. The

Fig. 2. Microscopic analysis of the esophagus and stomach of Burmese pythons (*Python molurus*). (A) Mucous epithelium of the esophagus of a fasting snake. (B, C) Anterior region of the stomach of a 1 day post feeding (DPF) snake. (D, E) Fundic region of the stomach from fasted and 1 DPF pythons, respectively. Note the presence of numerous fundic crypt openings. (F, G) Cross-sections of the fundic wall of a fasted and 1 DPF python, respectively. Note the enlarged crypt lumen in the fed snake. (H, I) Close view of the oxyntopeptic cell of a fasted and 1 DPF python, respectively, showing a dense apical tubulovesicular system in the fasting animal and elongated microvilli in the fed snake. Note the presence of numerous zymogen granules in the fasting animal and abundant mitochondria in the fed snake. (J) pyloric wall of a fasting animal with a mucus epithelium and wide sac glands underneath that are opened towards the gastric lumen. (A) Paraffin section; (B, D, E) environmental scanning electron micrographs; (C, F, G, J) emi-thin sections; (H, I) transmission electron micrographs. CL, crypt lumen; CO, crypt opening; Cr, crypt; Di, digitation; ECL, enlarged crypt lumen; F, folds; H, hair; L, lumen; MB, mucous bridge; mit, mitochohondria; N, nucleus; NG, neck gland; PG, pyloric gland; TVS, tubulovesicular system; ZG, zymogen granules.

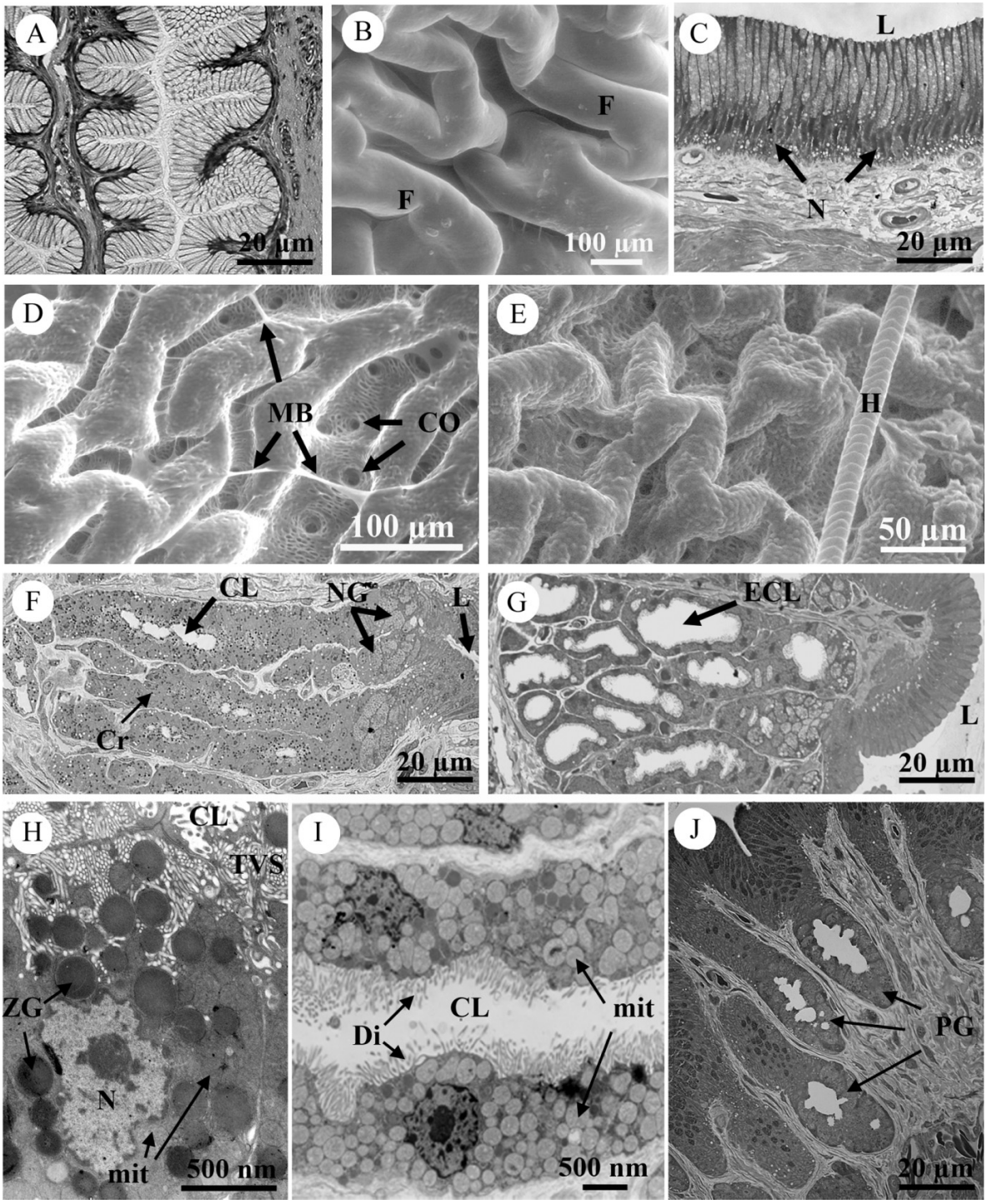

Fig. 3. Analysis of intestinal mucosa of Burmese pythons (*Python molurus*). (A) Scanning electron micrograph of a villus tip from the proximal intestine of a fasted python. Note the abundant cellular hypotrophy. (B, C) Transmission electron micrograph of the intestinal mucosa of a fasted python and after 1 day postfeeding (DPF), respectively. Note the pseudostratified epithelium in the fasting snake and the large vacuoles filling the cells and the basal nuclei in the simple columnar epithelium of the fed animal. (D) Unstained section at the tip of an intestinal villus of a 3 DPF snake viewed using DIC illumination. Note the presence of widened intercellular spaces. (E) Intestinal section stained with Sudan black of a 3 DPF snake. Note that the large vacuoles are stained indicating that they are filled with lipids. (F) Basal side of the intestinal mucosa 3 DPF. Lipid droplets are found inside the lamina propria. HC, hypotrophied cell; IS, intercellular spaces; L, lumen; LD, lipid droplet; LP, lamina propria; M, microvilli; N, nucleus; VT, villus tip.

snakes were fed laboratory mice and rats on a biweekly basis with each meal weighing ~25% of the snake's body mass. At the time of study, pythons weighted 661 ± 145 g (mean ± 1 SD) and were approximately 6 months old. Prior to experimentation, snakes were fasted for 40–50 days while still having access to water to ensure that they were postabsorptive (Secor and Diamond 1995). One set of fasting snakes (n = 4) was killed and the others fed rodent meals weighing ~25% of snake body mass and killed at 0.5, 1, 3, or 6 DPF (n = 4 or 5 per sampling period). One hour before being killed, each snake was injected intraperitoneally with a 50 mg/kg solution of 5-bromo-2′-deoxyuridine (BrdU; Sigma Chemicals, Saint Quentin Fallavier, France). Snakes were killed by decapitation and a mid-ventral incision was made to expose the internal organs. The stomach, small intestine, and large intestine were removed and flushed of any contents with ice-cold Ringers' solution. All housing and experimental procedures were conducted under animal care and used protocols approved by the Centre National de la Recherche Scientifique.

Scanning electron microscopy

Small tissues samples from the stomach (fundic and pyloric regions), small intestine (anterior region), and large intestine (anterior region) were fixed for 2 h at room temperature in 3% paraformaldehyde in 0.05 mol/L phosphate buffer (pH = 7.4) and subsequently dehydrated through a graded ethanol series. Samples were then bathed in 1,1,1,3,3,3-hexamethyldisilazane, and were subsequently air-dried and attached to specimen stubs with adhesive carbon tabs or silver paint. Samples were gold-coated (Edwards Sputter Coater, Manor Royal Crawley, England, UK) and examined with a Philips XL-30 ESEM in conventional mode (high vacuum) with a Thornley-Everhart secondary electron detector. To observe samples in the environmental mode of the XL-30 ESEM (wet mode), samples were fixed in 3% paraformaldehyde in buffered saline for 2 h at room temperature, washed in buffered saline, and immediately viewed while hydrated. Relative humidity at the sample surface was held at 80% by maintaining the specimen temperature at 4 °C and the sample chamber at 5 torr (1 torr = 133.322 Pa) of water vapor.

Light and transmission electron microscopy

Small samples of epithelium from the stomach (fundic and pyloric regions), small intestine (anterior and distal regions), and large intestine (anterior region) were fixed in 2.5% gluteraldehyde in 0.05 mol/L cacodylate buffer (pH = 7.4). Samples were subsequently postfixed in 1% osmium tetroxide, dehydrated in a graded ethanol series, and embedded in either Spurrs or Araldite 502 epoxy resin. Semithin (~1.5 μm) and ultra-thin sections (~90 nm) were placed on poly-L-lysine-coated slides or copper grids, respectively. Semi-thin sections were stained with toluidine blue or Sudan black following the Sire and Vernier protocol (Sire and Vernier 1980) and observed to describe postprandial changes in cell structure and organization. Ultra-thin sections were stained with uranyl acetate for 30 min and lead citrate for 3 min and examined with a Philips CM10 transmission electron microscope.

Cell replication

Stomach and small and large intestinal samples were fixed in 3% buffered paraformaldehyde, dehydrated in a graded ethanol series, and embedded in paraffin. Embedded tissues were sectioned (6 μm) and the sections placed on poly-L-lysine coated slides. Sections on slides were deparafinized, rehydrated, and incubated with 3% hydrogen peroxide for 10 min at 37 °C to inactivate endogenous peroxidase. Slides were then placed in 2 mol/L HCl for 30 min at 37 °C and then 0.1% trypsin 10 min at 37 °C. Sections were subsequently incubated for 15 min at room temperature in 5% normal goat serum and then treated with anti-BrdU (Sigma Chemicals) at 1:200 dilution for 2 h at 37 °C. They were then treated with biotinylated goat anti-mouse IgG (1:200) for 1 h at 37 °C and subsequently labeled with horseradish peroxidase conjugated extravidin (1:100) for 30 min at room temperature. Diamino-benzidine was used for color development (3 min incubation). Sections were mounted with Eukitt mounting medium and examined on a Zeiss Axioplan microscope. To quantify newly synthesized DNA of replicating cells, the BrdU-labeled cells (blocked in the S phase of the cellular cycle) were counted from a minimum of 10 sites from each section. For the stomach, the number of BrdU cells was quantified per crypt, whereas in the small and large intestine, stained cells were counted per micrometre of epithelium.

Morphometry, statistical analysis

To measure the crypt length and the height of the oxyntopeptic cells, longitudinal semithin sections of the fundic crypts were used. Crypt length was measured from the neck gland down to the bottom end of the crypts. Sections from four animals per nutritional condition were used to measure the length of 10 crypts and the height of 20 oxyntopeptic cells per snake. Along the crypts, only cells with apparent nuclei were measured from the basal membrane to the top of the cells, including the digitations. Data are presented as means ± SE. Statistical comparisons of experimental data were performed by one-way analysis of variance (ANOVA) and Tukey post hoc test using the software Sigmastat (Systat Software, Inc., San Jose, California, USA). The level of statistical significance was set at $P < 0.05$.

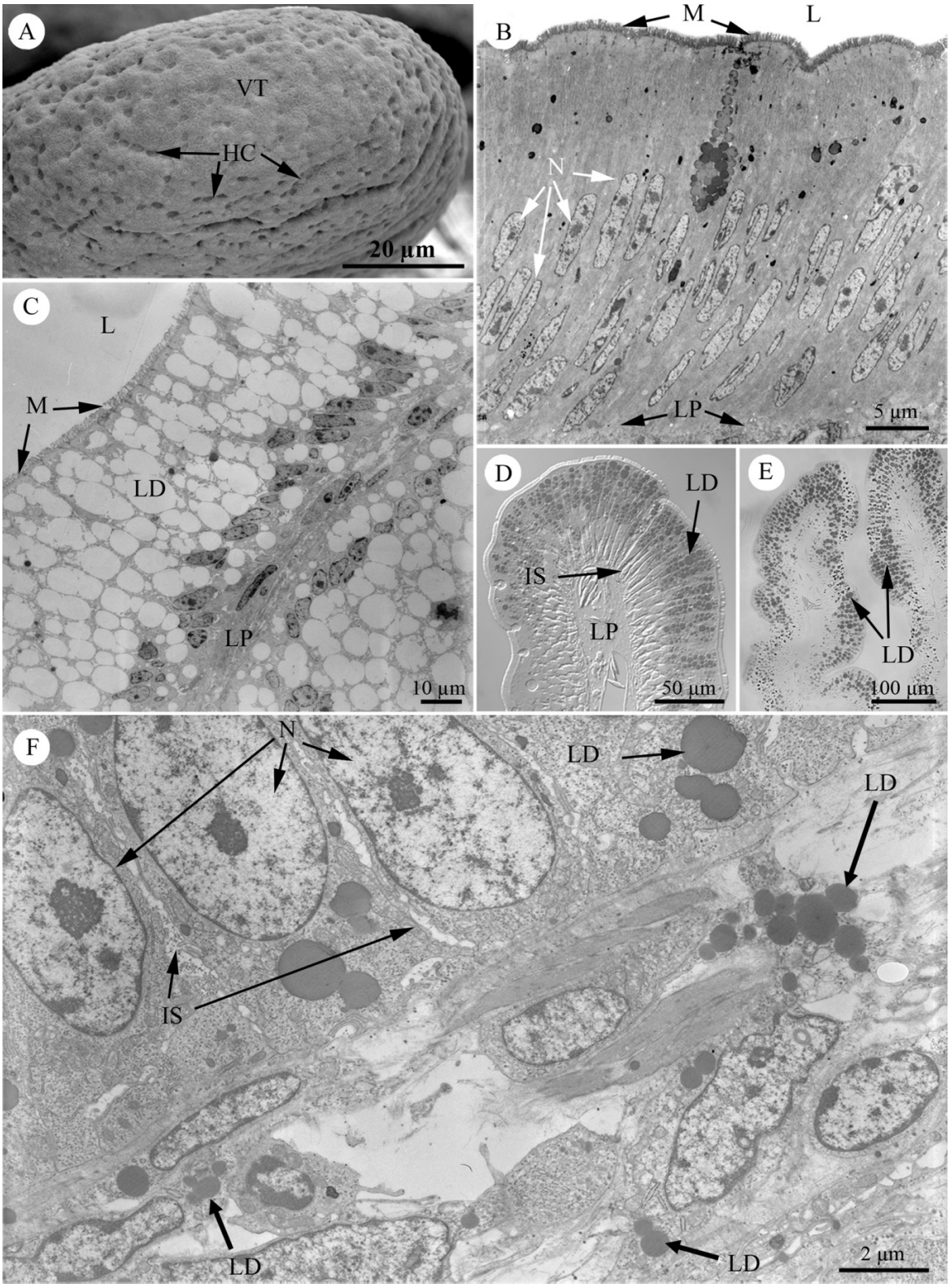

Results

Gross morphology and food passage

The digestive system of the Burmese pythons is composed of a straight, elongated esophagus that opens directly into the stomach with no esophageal sphincter (Figs. 1A, 1B, 1C), a pancreas and a gall bladder flanked at the start of the small intestine (Fig. 1C), a blind-end pouch, and finally, the cecum extending anteriorly to a large intestine and cloaca (Fig. 1C).

The stomach wall (Fig. 1D) possesses a thick fundic region lined with internal longitudinal folds (rugae) and a pyloric region anterior to a thick muscular pyloric sphincter. For the 4 fasted pythons, the stomach and small intestine

Fig. 4. Examination of mucosa of the colon of Burmese pythons (*Python molurus*). (A) Environmental scanning electron micrograph of the colonic epithelium. (B, C) Semi-thin sections of the colonic epithelium of a fasted python and after 1 DPF, respectively. Note the presence of numerous goblet cells, and of extended microvilli and enlarged intercellular spaces in the fed snake. (D, E) Transmission electron micrograph (TEM) of colonic ionocytes of a fasted python and after 1 DPF, respectively. Mitochondria-rich cells of the fasting snake are filled with lysosomes and large cytoplasmic bodies. (F) TEM of the basal side of the colonic epithelium of a 6 DPF snake. Epithelial cells possess numerous lipid droplets and glycogen. ICS, intercellular spaces; F, folds; G, glycogen; L, lumen; LD, lipid droplet; LE, late endosome; Lys, lysosomes; M, microvilli; MC, mucous cell; mit, mitochondria.

were empty, whereas for the 18 fed pythons, the large intestine and cecum contained unabsorbed material and fecal matter from the meal (Figs. 1E, 1F, 1G).

At 12 HPF, the rat meal had completely filled the stomach and the adjacent distal portion of the esophagus (Fig. 1E). By 1 DPF, ~30% of the rat had been broken down and passed into the small intestine (data not shown). At this time the small intestine had doubled in diameter and was partially filled with chyme. At 3 DPF, most of the rat meal (30%–50%) had passed from the stomach, resulting in the small intestine filling up with chyme, and all that remained of the rat in the stomach were portions of the lumbar regions, hind limbs, and tail (Fig. 1F). At 6 DPF, only small mats of hair were present in the stomach. The small intestine contained a small amount of chyme, but the large intestine and cecum were almost completely filled with unabsorbed material and fecal matter (Fig. 1D).

Gastric and intestinal epithelium

The luminal surface of the gastric epithelium (Figs. 2A, 2B, 2C) possesses numerous openings (Figs. 2D, 2E) beneath which are the gastric pits. The upper regions of the crypts (neck region) are lined with mucous cells, whereas the deeper epithelium (pit region) contains numerous mitochondria-rich oxyntopeptic cells (Figs. 2F, 2G). that are responsible for the production of both pepsinogen (precursor of the peptidase, pepsin) and HCl.

When fasted, the oxyntopeptic cells of pythons possess numerous zymogen granules and a thick apical tubulovesicular system (Fig. 2H). After feeding, there is a transformation of the oxyntopeptic cells and a reduction in the tubulovesicular system that is accompanied by the development of elongated digitations in the apical membrane extending into the crypt lumen (Fig. 2I). In addition, the oxyntopeptic cells contain fewer zymogen granules, which are concentrated just beneath the apical surface (Fig. 2I). By 3 DPF, there is a restoration of the apical tubulovesicular system and an increase in the number of zymogen granules henceforth concentrated at the cell's basal end. After 6 DPF, as the last of meal remnants exit the stomach, the gastric epithelium already begins to return to the fasting condition.

For the pyloric region of the stomach, the gastric glands located underneath the mucous epithelium do not present evident morphological changes between fasting and feeding conditions. They appear as epithelial invaginations, do not contain elongated crypts. They possess goblet cells with the same characteristics as the neck cells found farther up in the stomach (Fig. 2J).

The epithelial lining within the anterior small intestine of fasted pythons is composed largely of tightly packed enterocytes whose nuclei are positioned in slightly different planes resulting in the appearance of a pseudostratified epithelium (Fig. 3B). Within 12 HPF, the enterocytes begin to widen, resulting in a change of appearance from a pseudostratified epithelium to a simple columnar epithelium (Fig. 3B), an orientation that is maintained throughout digestion. After feeding, we observed the presence of large vacuoles filled with lipids within enterocytes (detected by staining with Sudan black), and larger spaces between adjoining cells at the basal region of cells (Figs. 3D, 3E). At 6 DPF, lipid droplets were only observed at the basal region of the enterocytes (Fig. 3F).

The anterior large intestine of both fasted and fed Burmese pythons is characterized by a folded luminal surface and an epithelium composed of tall columnar and monolayered enterocytes interspersed by numerous goblet cells (Figs. 4A, 4B). While we did not observe any postprandial changes in the dimensions of these enterocytes, the microvilli of these cells doubled in length and there was an increase in space between enterocytes after feeding (Fig. 4C). Feeding also resulted in an increase in the amount of primary lysosomes and late endosomes (Fig. 4D). Glycogen and lipid droplets were also observed at the basal side of these enterocytes (Figs. 4D, 4E, 4F).

Finally, while numerous primary lysosomes characterize most of the enterocytes of the small intestine in fasting animals (Fig. 3B), other endocytotic organelles were observed for the 3 DPF and 6 DPF pythons within the mucosal cells of the stomach and intestine (Figs. 5A–5I). Among these, sorting endosomes and multivesicular bodies (MVB) were observed in various stages of maturation next to the apical surface of the cells (Figs. 5A, 5B). These endosomes possess an outer double membrane and contain many small intraluminal membrane-bound vesicles forming from invaginations of the outer membrane (Figs. 5C–5E). Multilamellar bodies (MLB) (Figs. 5F, 5G) and lysosomes (Fig. 5H) were also observed distributed along the full length of the cells (Fig. 5I). They can fuse to pre-existing homogenous lysosomes (Figs. 5F, 5G) to form polymorphic and heterogeneous masses. Some of these can then be taken up and degraded by intraepithelial macrophages (Fig. 5J). Others are expelled from the cells and carried via the intercellular spaces (Fig. 5K) to the lamina propria.

Morphometry

In fasting pythons, crypts appeared elongated but were reduced in length immediately after feeding (ANOVA, $F_{[2,50]} = 15.06$, $p < 0.001$). Then, crypt length lengthened 1 and 3 DPF (Fig. 6A). The height of the oxyntopeptic cells also appears to be related to the morphological reshaping of the cells and is dependent on the feeding status of the animals (Fig. 6B). The differences observed between feeding groups are statistically significant (ANOVA, $F_{[1,84]} = 47.44$, $p < 0.001$). The Tukey post hoc test indicates that cells from

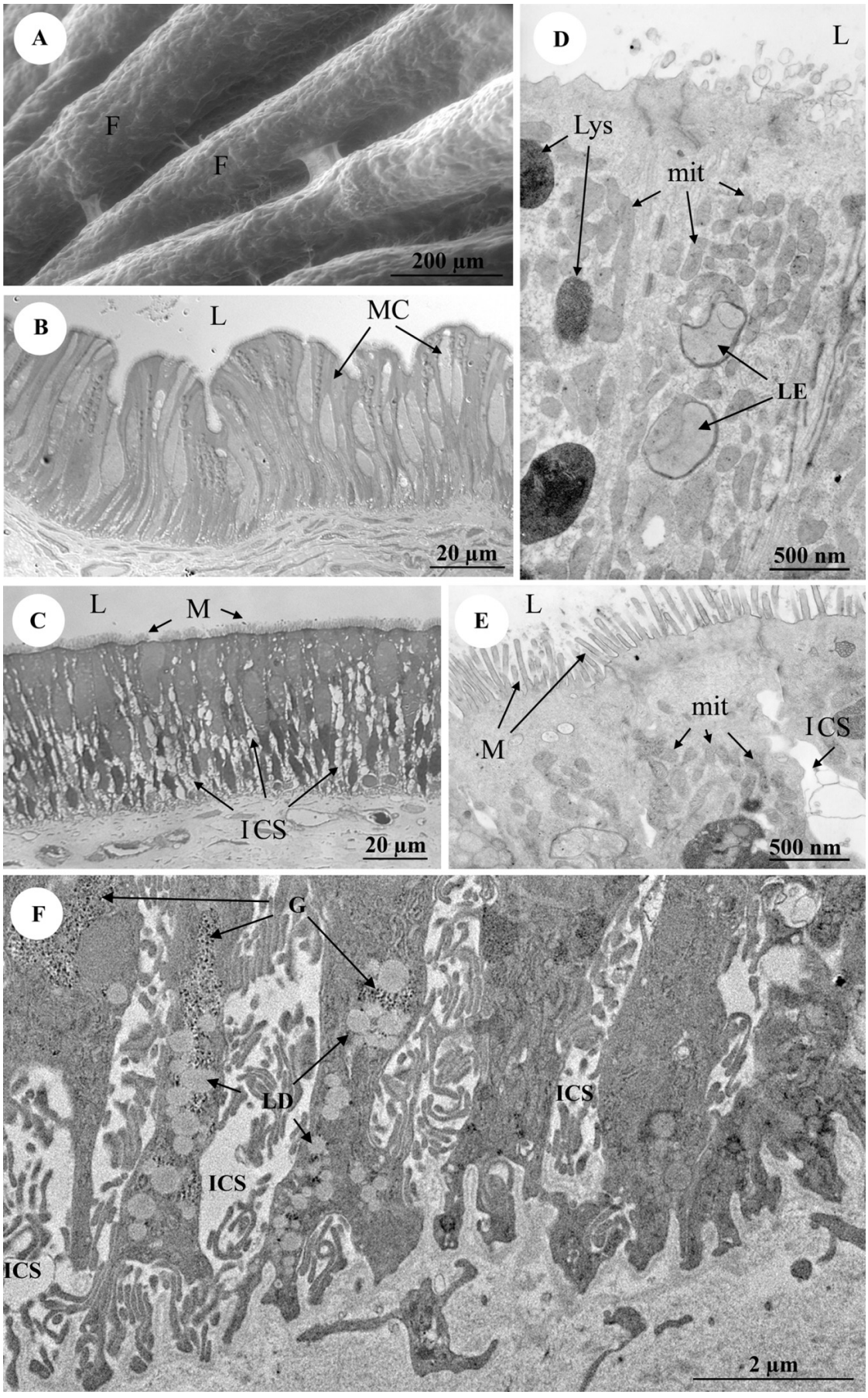
A
F
F
200 µm
B
L
MC
20 µm
C
L
M
ICS
20 µm
D
L
Lys
mit
LE
500 nm
E
L
M
mit
ICS
500 nm
F
G
LD
ICS
ICS
ICS
2 µm

Fig. 5. Analysis of intracellular bodies of Burmese pythons (*Python molurus*). (A) Multivesicular bodies (MVBs) located on the apical side of an oxyntopeptic cell (1 day postfeeding (DPF)). (B, C, D, E) Sorting endosomes and MVBs located on the apical side of intestinal enterocytes and colon at different stages of maturation (12 h postfeeding (HPF), 1, 3, and 6 DPF), respectively. (F, G) Multilamellar bodies fusing with MVBs within an oxyntopeptic cell and intestinal enterocyte, respectively (3 and 6 DPF). (H) Large lysosome (3 DPF). (I) Basal side of mitochondria-rich cells of the colon interspaced by large intercellular spaces and containing large lipid droplets, as well as late endosomes and lysosomes (3 DPF). (J) Intraepithelial macrophage engulfing late lysosomes (arrows) in proximal intestine (6 DPF). (K) Intercellular space filled with late lysosomes (arrows). Di, apical digitations; ICP, intercellular space; Lys, lysosomes; mit, mitochondria; MC, mucous cell; MLB, multilamellar body; MP, intraepithelial macrophage; MV, microvilli; N, nucleus; SE, sorting endosome; TVS, tubulovesicular system; V, formation of vesicles from the membrane of MVBs.

fasting snakes are taller than cells from the postfed snake samples and that 12 HPF snakes have the shortest oxyntopeptic cells (Fig. 6B).

Cell renewal

For the fundic region of the stomach, the anterior small intestine, and the anterior large intestine, the relative number of cells undergoing replication varied significantly among fasted and postfeeding periods (Figs. 7A–7C). For the stomach, we did not detect replication of any cells along the upper or lower regions of the pit glands for either fasted snakes or at 12 HPF (Fig. 7A). The first observation of replicating cells was seen at 1 DPF, but only along the upper portions of the crypts (Fig. 7A micrograph). The number of replication cells for this region of the crypts continued to increase through 3 DPF and 6vDPF. We did not observe any cell replication within the lower pit regions of the crypts over the 6 days of digestion. Unlike the stomach, the mucosa of the anterior small intestine in fasted Burmese pythons contained a scattering of replicating cells (Fig. 7B). Such cells appeared randomly distributed across the epithelium surface (Fig. 7B micrograph). Within 12 HPF, the number of replication cells quadrupled, and by 1 DPF, the number had increased almost 10-fold (Fig. 7B). The number of epithelial cells undergoing replication peaked at 3 DPF at 23 times fasted levels and did not show any significant change by 6 DPF (Fig. 7B). The large intestine of fasted Burmese pythons also possessed cells undergoing replication. Feeding triggered a doubling in replication within 12 HPF and a 13-fold increase within 1 DPF (Fig. 7C). The density of replicating cells of the large intestinal epithelium reached a plateu at 1 DPF, remained the same at 3 DPF, and slightly began decreasing at 6 DPF. Among these three tissues, there was an apparent positional gradient in the density of replicating cells during digestion. The number of cells undergoing replication per length of epithelium for the small and large intestines was 13 and 50 times greater, respectively, than that observed for the fundic region of the stomach.

Discussion

The phenotypic plasticity of the python's gut with feeding and fasting is manifested in the stomach, by the upregulation and downregulation of cellular performance (acid production, enzyme activities, etc.) (Secor et al. 2000), as well as a reorganization of the fundic pits and oxyntopeptic cells (or pit cells) within hours after feeding (this study). These cells, typical of nonmammalian species (Sedar 1961; Ito 1967; Giraud et al. 1979), undergo profound morphological changes when stimulated to secrete HCl by the presence of food inside the stomach. The overall height of the cell is reduced upon production of HCl, enzymes, and by the depletion of intracellular glycogen stores. Their apical surface is greatly expanded compared with nonsecreting ones, owing to the fusion of cytoplasmic tubulovesicular membranes with the apical membrane surface (Forte et al. 1980). Within hours after the ingestion of the prey, stored zymogen granules containing the inactive enzyme precursor pepsinogen (i.e., proenzyme) move apically within the oxyntopeptic cells and reach the gastric lumen. In mammals, these processes appear similar but are separated into two distinct cellular types, namely, chief cells (or peptic cells), containing zymogen granules, and parietal cells (or oxyntic cells) that possess an extensive secretory network (or intracellular canaliculi), and cytoplasmic tubulovesicles (or tubulovesicular membrane system) (Ogata and Yamasaki 2000). In resting oxyntic cells, there are many tubulovesicles but a limited intracellular canalicular surface, whereas in active cells, there is an increase of the intracellular canaliculus. Oxyntopeptic cells can also be found in mammals under specific conditions, for instance in the fundic glands of humans with chronic gastritis (Sharov 1973).

Within the small intestine, it is now well-established that mucosal cells of fasting pythons are arranged in a pseudostratified fashion (Starck and Beese 2001; Lignot et al. 2005). In fed animals, however, the mucosal cells become monolayered with numerous and large intracytoplasmic lipid droplets accumulating within the enterocytes (Starck and Beese 2001); these droplets are especially abundant at the tip and along the thin edges of the villi (Lignot et al. 2005). These neutral lipids enter the cells through endocytosis, are surrounded by an amphiphatic monolayer of lipids that corresponds to a single-membrane leaflet (Murphy 2001; Martin and Parton 2006; Söllner 2007), and move down through the cells until they reach the basolateral membranes. This is similar to what has been described for mammals, but the magnitude of this uptake has only been described in refed fish, amphibians, and other snake species (Noaillac-Depeyre and Gas 1974, 1979; Sire et al. 1981; Starck and Beese 2002; Cramp and Franklin 2003).

In the colon, the mitochondria-rich cells that are interspersed with goblet cells change morphology based on the feeding status of the snake. Microvilli length increases after feeding and large intercellular spaces appear. Also, glycogen and lipid droplets are found within the mitochondria-rich absorbing cells next to the basal membrane. Another feature is the abundance of early and late endosomes, lamellar bodies (multilamellar lysosomes, MLL), and primary and secondary lysosomes. These MLL also are found in the gastric and small intestinal cells of fasting and postfed pythons that are

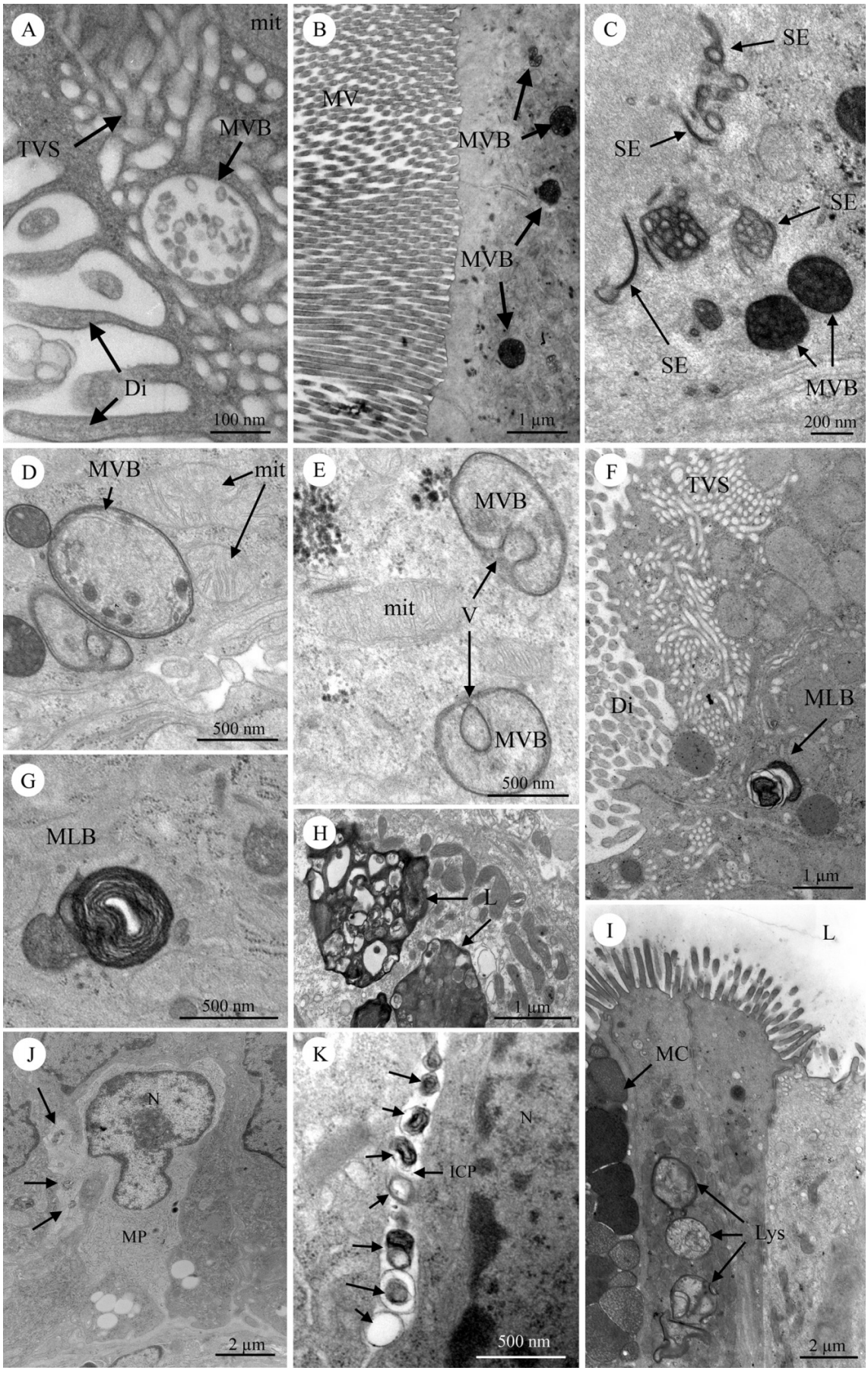
A
mit
TVS
MVB
Di
100 nm
B
MV
MVB
MVB
1 µm
C
SE
SE
SE
SE
MVB
200 nm
D
MVB
mit
500 nm
E
MVB
mit
V
MVB
500 nm
F
TVS
Di
MLB
1 µm
G
MLB
500 nm
H
L
1 µm
I
L
MC
Lys
2 µm
J
N
MP
2 µm
K
N
lCP
500 nm

Fig. 6. (A) Fundic crypt length (in μm) of fasted, 12 h post feeding (HPF), 1 day postfeeding (DPF), 3 DPF, and 6 DPF Burmese pythons (*Python molurus*) measured from the neck gland located just below the mucous epithelium down to the bottom end of the crypts. (B) Heights of the oxyntopeptic cells and apical digitations. Only cells with apparent nuclei were measured. Four animals per nutritional condition were used.

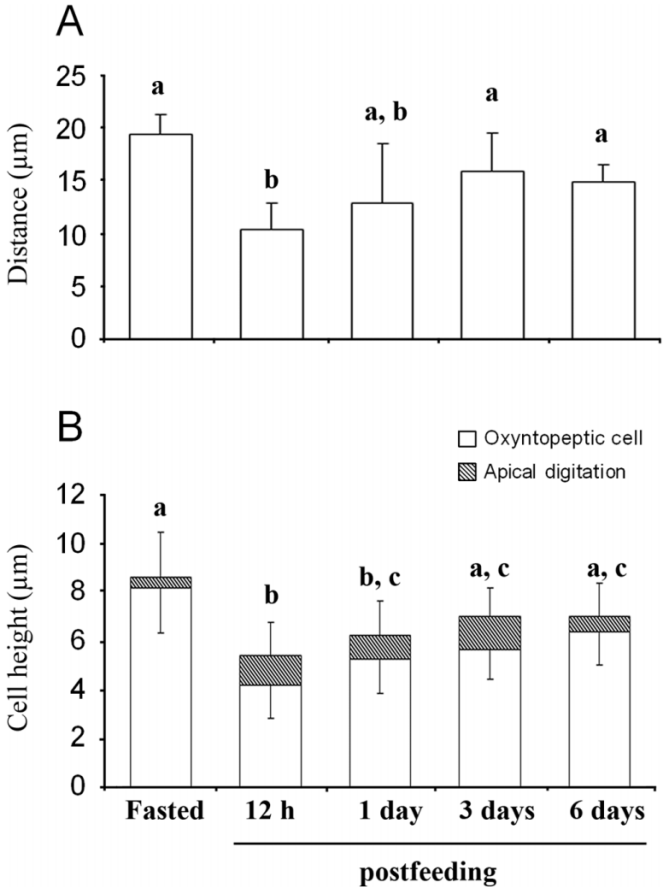

in the second part of the postprandial period. They regulate the composition of the cell and separate proteins that will recycle to other cellular compartments from those that will be degraded in lysosomes. For this recycling, a maturation process must occur from early to late endosomes and lysosomes (Stahl and Barbieri 2002; Gruenberg and Stenmark 2004). This is initiated by supranuclear membrane-bound multivesicular endosomes or multivesicular bodies (MVB). While recycled integral membrane proteins and lipids are removed back to the trans-Golgi network and plasma membrane, proteins destined for degradation are incorporated into intraluminal vesicles that bud from the MVB-limiting membrane. These vesicles are then degraded when MVBs fuse with lysosomes. Gastric and intestinal cells in fasting pythons also contain large multilamellar bodies (lamellar lysosome) possessing multiple concentric membrane layers. In mammals, these MLLs are usually found in the lung epithelium where they provide a storage form for the lung surfactant (Stahlman et al. 2000), as well as in the gastrointestinal tract, tongue papillae, oral epithelium, and mucosa cells of the stomach where their principal functions are storage and secretion of lipids (Schmitz and Müller 1991). The presence of these MLLs in the enterocytes indicates that a great amount of recycling occurs for the membranes used for nutrient and particularly lipid uptake between each feeding bout. Finally, while supranuclear primary lysosomes are numerous in the gastrointestinal lining of fasting pythons, secondary lysosomes that are heterogeneous in morphology are mostly found in digesting pythons. As in mammals, they represent the terminal compartment of the recycling pathway. Therefore, and as already described, one hypothesis is that lysosomes can fuse with the numerous late endosomes present in the enterocytes and can be reused in subsequent cycles of fusion, digestion, and reformation (Bright et al. 1997; Luzio et al. 2003). Some of these lysosomes can also be expelled from the enterocytes into the intercellular spaces. They are either taken up by intraepithelial macrophages or moved farther into the intestinal submucosa where they will also eventually be recycled by the numerous macrophages present.

It is also evident from this study that the rate of cell replication is modulated according to the snake's digestive status. It increases moderately within hours after feeding and levels off within a few days, the timing of which is organ-specific. For the stomach, it starts following ingestion and peaks ~3 DPF. Considering the elevated workload on the python's oxyntopeptic cells, namely continuous H^+ pumping and pepsinogen release over a few days, it is not surprising that these cells need to be replaced soon after feeding. A similar region for cell proliferation (between the surface and mucus cells of the neck portion of the gastric gland), as observed here for Burmese pythons, has also been noted for African clawed frogs (*Xenopus laevis* (Daudin, 1802)) (Oinuma et al. 1992) and for mammals (Willems 1972; Kataoka et al. 1984). For instance, gastric cell proliferation appeared greater in fed Norway rats (*Rattus norvegicus* (Berkenhout, 1769)) than in fasted individuals (Hunt 1957). Similarly, in the intestine, the peak in enterocyte replication occurs during peaks in digestive performance (Cox and Secor 2008). This proliferation is randomly distributed along the intestinal villi and is similar to what has been reported for the winter flounder (*Pseudopleuronectes americanus* (Walbaum, 1792)) (Trier and Moxey 1980). For this fish, gastric cell proliferation is also greater for fed compared with fasted individuals, and is not compartmentalized to the base of the folds and interfolds epithelium (intervillus pockets) as seen in the zebrafish (*Brachydanio rerio* (Hamilton, 1822)) and other species of teleosts (Noaillac-Depeyre and Gas 1974; Stroband and Debets 1978; Rombout et al. 1984; Ng et al. 2005). Interestingly, in the neotenic cave salamander (*Proteus anguinus* Laurenti, 1768), clusters of dividing cells responsible for the intestinal renewal are situated directly below the epithelium (Bizjak Mali and Bulog 2004). Similar subepithelial buds or "cell nests" are present in the salamanders *Triturus vulgaris* (currently known as *Lissotriton vulgaris* (L. 1758)) and *Necturus maculosus* (Rafinesque, 1818) (O'Steen and Walker 1960; Patten 1960), as well as in a very limited area along the intestinal length of the freshwater painted turtle, *Chrysemys picta* (Schneider, 1783) (Wurth and Musacchia 1964). This compartmentization is even more pronounced in crocodilians (Kotzé et al. 1992; Starck et al. 2007), birds (Uni et al. 1998; Starck 1996; Geyra et al. 2001), and mammals (Wilson and Potten

Fig. 7. Cellular replication indicated by 5-bromo-2′-deoxyuridine (BrdU) incorporation in fasted, 12 h postfeeding (HPF), 1 DPF, 3 DPF, and 6 DPF Burmese pythons (*Python molurus*). Examination of BrdU incorporation in mucosal cells of (A) fundic regions of the stomach, (B) proximal intestine, and (C) colon. The rate of mitosis increases slowly with feeding, then reaches a plateau 1–6 DPF according to the organ examined. Values are means ± SD. Letters indicate significant differences among mean values (Tukey post hoc test, $\alpha = 0.05$). Micrographs are examples from 3 DPF pythons. C, crypt; L, lumen; NG, neck gland; SN, stained nuclei.

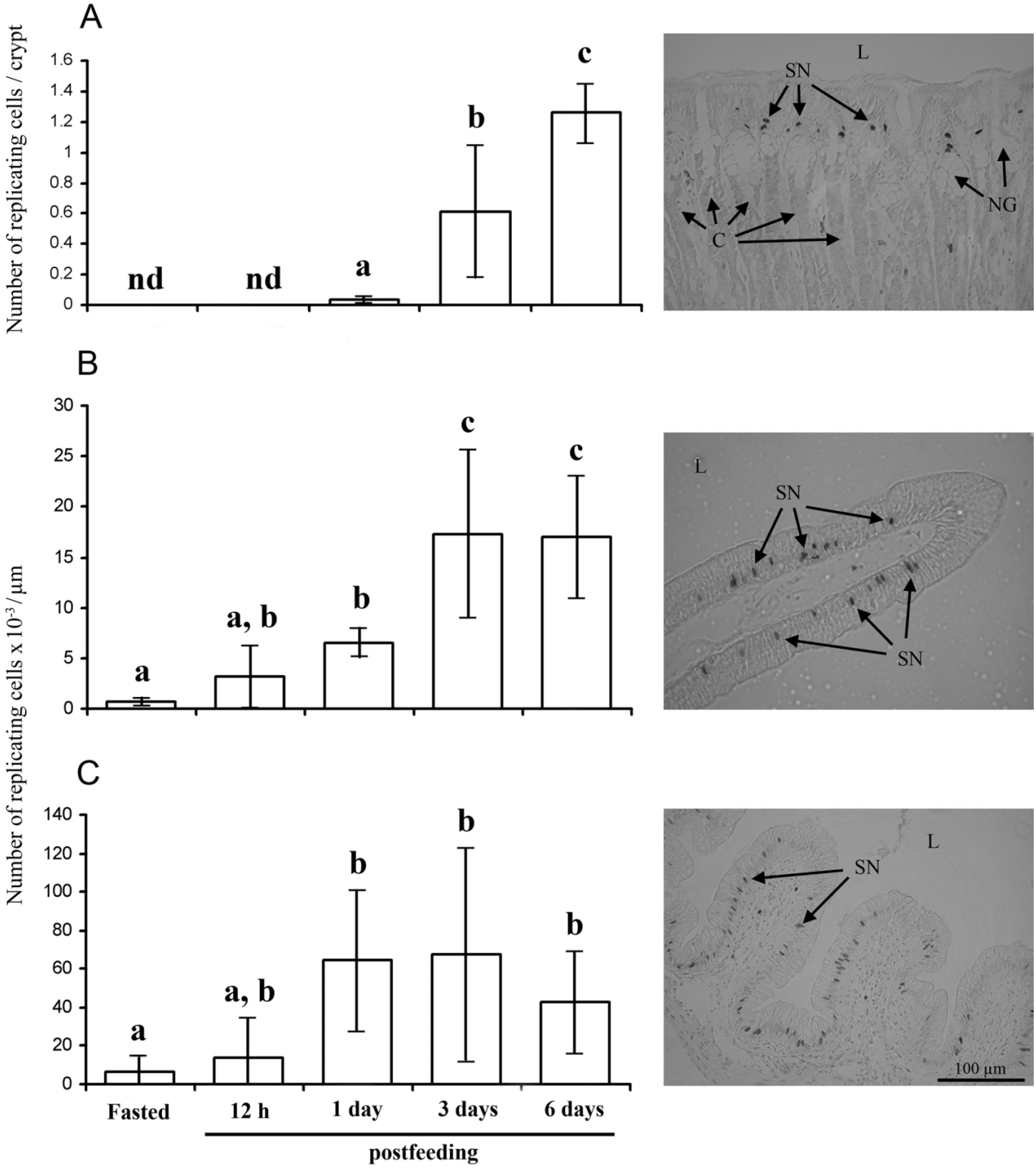

2004), with cell proliferation occurring within crypts of Lieberkühn located at the bases of the villi (Aldewachi et al. 1975). For the large intestine, both fasted and fed pythons experience cell replication, with the greatest concentration of replicating enterocytes observed at 1 and 3 DPF. Surprisingly, and for each time point considered after feeding, this process occurs at a higher rate in the large intestine than in the small intestine.

Therefore, cell turnover and remodelling of the mucosal cells induce an inherent cost of upregulation and downregulation of the digestive system in Burmese pythons. Before the completion of the postprandial period, these cells undergo profound recycling. Also, the peak in cell replication occurs during peaks in digestive performance. As some mucosal cells are literally "worn out" because of their elevated activity, they must be replaced. These new cells may assist in the completion of digestion and absorption, but must rapidly undergo downregulation, remaining semidormant until the next meal. With the next feeding bout, they will grow and upregulate their functions and may, or may not, be replaced during digestion. This cellular plasticity adjoined with cell renewal allows the digestive system to anticipate the next feeding bout and constitutes a spectacular example of the phenotypic plasticity that can occur in an organism adapted to infrequent feeding.

Acknowledgements

We are grateful to A. Ackermann for his technical expertise in histology. Robert K. Pope was supported by a Fullbright – Alsace Regional Council Award.

References

Aldewachi, H.S., Wright, N.A., Appleton, D.R., and Watson, A.J. 1975. The effect of starvation and refeeding on cell population kinetics in the rat small bowel mucosa. J. Anat. **119**(1): 105–121. PMID:1133081.

Altmann, G.G. 1972. Influence of starvation and refeeding on mucosal size and epithelial renewal in the rat small intestine. Am. J. Anat. **133**(4): 391–400. doi:10.1002/aja.1001330403. PMID: 5016502.

Bizjak Mali, L., and Bulog, B. 2004. Histology and ultrastructure of the gut epithelium of the neotenic cave salamander, *Proteus anguinus* (Amphibia, Caudata). J. Morphol. **259**(1): 82–89. doi:10.1002/jmor.10171. PMID:14666527.

Bright, N.A., Reaves, B.J., Mullock, B.M., and Luzio, J.P. 1997. Dense core lysosomes can fuse with late endosomes and are reformed from the resultant hybrid organelles. J. Cell Sci. **110**(17): 2027–2040. PMID:9378754.

Buts, J.-P., Vijverman, V., Barudi, C., De Keyser, N., Maldague, P., and Dive, C. 1990. Refeeding after starvation in the rat: comparative effects of lipids, proteins and carbohydrates on jejunal and ileal mucosal adaptation. Eur. J. Clin. Invest. **20**(4): 441–452. doi:10.1111/j.1365-2362.1990.tb01882.x. PMID: 2121504.

Carey, H.V. 1990. Seasonal changes in mucosal structure and function in ground squirrel intestine. Am. J. Physiol. **259**(2): R385–R392. PMID:2386247.

Cox, C.L., and Secor, S.M. 2008. Matched regulation of gastrointestinal performance in the Burmese python, *Python molurus*. J. Exp. Biol. **211**(7): 1131–1140. doi:10.1242/jeb.015313. PMID: 18344488.

Cramp, R.L., and Franklin, C.E. 2003. Is re-feeding efficiency compromised by prolonged starvation during aestivation in the green striped burrowing frog, *Cyclorana alboguttata*? J. Exp. Zool. **300A**(2): 126–132. doi:10.1002/jez.a.10272.

Dou, Y., Gregersen, S., Zhao, J., Zhuang, F., and Gregersen, H. 2001. Effect of re-feeding after starvation on biomechanical properties in rat small intestine. Med. Eng. Phys. **23**(8): 557–566. doi:10.1016/S1350-4533(01)00091-1. PMID:11719078.

Dunel-Erb, S., Chevalier, C., Laurent, P., Bach, A., Decrock, F., and Le Maho, Y. 2001. Restoration of the jejunal mucosa in rats refed after prolonged fasting. Comp. Biochem. Physiol. A Mol. Integr. Physiol. **129**(4): 933–947. doi:10.1016/S1095-6433(01)00360-9.

Forte, J.G., Machen, T.E., and Öbrink, K.J. 1980. Mechanisms of gastric H^+ and Cl^- transport. Annu. Rev. Physiol. **42**(1): 111–126. doi:10.1146/annurev.ph.42.030180.000551. PMID:6250451.

Geyra, A., Uni, Z., and Sklan, D. 2001. The effect of fasting at different ages on growth and tissue dynamics in the small intestine of the young chick. Br. J. Nutr. **86**(1): 53–61. doi:10.1079/BJN2001368. PMID:11432765.

Giraud, A.S., Yeomans, N.D., and St. John, D.J.B. 1979. Ultrastructure and cytochemistry of the gastric mucosa of a reptile, *Tiliqua scincoides*. Cell Tissue Res. **197**(2): 281–294. doi:10.1007/BF00233920. PMID:436148.

Gruenberg, J., and Stenmark, H. 2004. The biogenesis of multivesicular endosomes. Nat. Rev. Mol. Cell Biol. **5**(4): 317–323. doi:10.1038/nrm1360. PMID:15071556.

Hunt, T.E. 1957. Mitotic activity in the gastric mucosa of the rat after fasting and refeeding. Anat. Rec. **127**(3): 539–550. doi:10.1002/ar.1091270305. PMID:13425013.

Ito, S. 1967. Anatomic structure of the gastric mucosa. *In* Handbook of physiology. Section 6, Vol. 2. *Edited by* U.S. Heidel and C.F. Code. American Physiological Society, Baltimore, Md. pp. 705–741.

Kataoka, K., Sakano, Y., and Miura, J. 1984. Histogenesis of the mouse gastric mucosa, with special reference to type and distribution of proliferative cells. Arch. Histol. Jpn. **47**(5): 459–474. doi:10.1679/aohc.47.459. PMID:6532366.

Kotzé, S.H., Van der Merwe, N.J., Van Aswegen, G., and Smith, G.A. 1992. A light microscopical study of the intestinal tract of the Nile crocodile (*Crocodylus niloticus*, Laurenti 1768). Onderstepoort J. Vet. Res. **59**(4): 249–252. PMID:1297954.

Lignot, J.-H., Helmstetter, C., and Secor, S.M. 2005. Postprandial morphological response of the intestinal epithelium of the Burmese python (*Python molurus*). Comp. Biochem. Physiol. A Mol. Integr. Physiol. **141**(3): 280–291. doi:10.1016/j.cbpb.2005.05.005.

Luzio, J.P., Poupon, V., Lindsay, M.R., Mullock, B.M., Piper, R.C., and Pryor, P.R. 2003. Membrane dynamics and the biogenesis of lysosomes (Review). Mol. Membr. Biol. **20**(2): 141–154. doi:10.1080/0968768031000089546. PMID:12851071.

Martin, S., and Parton, R.G. 2006. Lipid droplets: a unified view of a dynamic organelle. Nat. Rev. Mol. Cell Biol. **7**(5): 373–378. doi:10.1038/nrm1912. PMID:16550215.

Murphy, D.J. 2001. The biogenesis and functions of lipid bodies in animals, plants and microorganisms. Prog. Lipid Res. **40**(5): 325–438. doi:10.1016/S0163-7827(01)00013-3. PMID:11470496.

Ng, A.N., de Jong-Curtain, T.A., Mawdsley, D.J., White, S.J., Shin, J., Appel, B., Dong, P.D., Stainier, D.Y., and Heath, J.K. 2005. Formation of the digestive system in zebrafish: III. Intestinal epithelium morphogenesis. Dev. Biol. **286**(1): 114–135. doi:10.1016/j.ydbio.2005.07.013. PMID:16125164.

Noaillac-Depeyre, J., and Gas, N. 1974. Fat absorption by the en-

terocytes of the carp (*Cyprinus carpio* L.). Cell Tissue Res. **155**(3): 353–365. doi:10.1007/BF00222811. PMID:4376459.

Noaillac-Depeyre, J., and Gas, N. 1979. Structure and function of the intestinal epithelial cells in the perch (*Perca fluviatillis* L.). Anat. Rec. **195**(4): 621–627. doi:10.1002/ar.1091950405. PMID: 525830.

O'Steen, W.K., and Walker, B.E. 1960. Radioautographic studies of regeneration in the common newt. 1. Physiological regeneration. Anat. Rec. **137**(4): 501–509. doi:10.1002/ar.1091370409. PMID:13730117.

Ogata, T., and Yamasaki, Y. 2000. Morphological studies on the translocation of tubulovesicular system toward the intracellular canaliculus during stimulation of the gastric parietal cell. Microsc. Res. Tech. **48**(5): 282–292. doi:10.1002/(SICI)1097-0029(20000301)48:5<282::AID-JEMT5>3.0.CO;2-H. PMID: 10700045.

Oinuma, T., Kawano, J., and Suganuma, T. 1992. Bromodeoxyuridine-immunohistochemistry on cellular differentiation and migration in the fundic gland of *Xenopus laevis* during development. Cell Tissue Res. **269**(2): 205–212. doi:10.1007/BF00319610. PMID:1423489.

Patten, S.F., Jr. 1960. Renewal of the intestinal epithelium of the Urodele. Exp. Cell Res. **20**(3): 638–641. doi:10.1016/0014-4827(60)90146-4. PMID:13733361.

Rombout, J.H., Stroband, H.W., and Taverne-Thiele, J.J. 1984. Proliferation and differentiation of intestinal epithelial cells during development of *Barbus conchonius* (Teleostei, Cyprinidae). Cell Tissue Res. **236**(1): 207–216. doi:10.1007/BF00216533. PMID: 6713508.

Schmitz, G., and Müller, G. 1991. Structure and function of lamellar bodies, lipid–protein complexes involved in storage and secretion of cellular lipids. J. Lipid Res. **32**(10): 1539–1570. PMID:1797938.

Secor, S.M., and Diamond, J. 1995. Adaptive responses to feeding in Burmese pythons: pay before pumping. J. Exp. Biol. **198**(6): 1313–1325. PMID:7782719.

Secor, S.M., and Diamond, J. 1997. Effects of meal size on postprandial responses in juvenile Burmese pythons (*Python molurus*). Am. J. Physiol. **272**(3): R902–R912. PMID:9087654.

Secor, S.M., Whang, E.E., Lane, J.S., Ashley, S.W., and Diamond, J. 2000. Luminal and systemic signals trigger intestinal adaptation in the juvenile python. Am. J. Physiol. **279**: G1177–G1187.

Sedar, A.W. 1961. Electron microscopy of the oxyntic cell in the gastric glands of the bullfrog, *Rana catesbiana*. II. The acid-secreting gastric mucosa. J. Biophys. Biochem. Cytol. **10**: 47–57. PMID:13749582.

Sharov, V.G. 1973. Cells with features of chief and parietal cells inthe human gastric mucosa in chronic gastritis. Bull. Exp. Biol. Med. **75**: 717–719.

Sire, M.F., and Vernier, J.M. 1980. Lipid staining on semithin sections with sudan black B or nile blue sulphate. Application to intestinal fat absorption. Acta Histochem. Cytochem. **13**(2): 193–201.

Sire, M.F., Lutton, C., and Vernier, J.M. 1981. New views on intestinal absorption of lipids in teleostean fishes: an ultrastructural and biochemical study in the rainbow trout. J. Lipid Res. **22**(1): 81–94. PMID:7217788.

Söllner, T.H. 2007. Lipid droplets highjack SNAREs. Nat. Cell Biol. **9**(11): 1219–1220. doi:10.1038/ncb1107-1219. PMID: 17975543.

Stahl, P.D., and Barbieri, M.A. 2002. Multivesicular bodies and multivesicular endosomes: the "ins and outs" of endosomal traffic. Sci. STKE, **16**(141): pe32.

Stahlman, M.T., Gray, M.P., Falconieri, M.W., Whitsett, J.A., and Weaver, T.E. 2000. Lamellar body formation in normal and surfactant protein B-deficient fetal mice. Lab. Invest. **80**(3): 395–403. PMID:10744075.

Starck, J.M. 1996. Intestinal growth in altricial European starling (*Sturnus vulgaris*) and precocial Japanese quail (*Coturnix coturnix japonica*): a morphometric and cytokinetic study. Acta Anat. (Basel), **156**(4): 289–306. doi:10.1159/000147857. PMID: 9078400.

Starck, J.M., and Beese, K. 2001. Structural flexibility of the intestine of Burmese python in response to feeding. J. Exp. Biol. **204**(2): 325–335. PMID:11136618.

Starck, J.M., and Beese, K. 2002. Structural flexibility of the small intestine and liver of garter snakes in response to feeding and fasting. J. Exp. Biol. **205**(10): 1377–1388. PMID:11976350.

Starck, J.M., Cruz-Neto, A.P., and Abe, A.S. 2007. Physiological and morphological responses to feeding in broad-nosed caiman (*Caiman latirostris*). J. Exp. Biol. **210**(12): 2033–2045. doi:10.1242/jeb.000976. PMID:17562877.

Stroband, H.W., and Debets, F.M. 1978. The ultrastructure and renewal of the intestinal epithelium of the juvenile grasscarp, *Ctenopharyngodon idella* (Val.). Cell Tissue Res. **187**(2): 181–200. doi:10.1007/BF00224364. PMID:630592.

Trier, J.S., and Moxey, P.C. 1980. Epithelial cell proliferation in the intestine of the winter flounder, *Pseudopleuronectes americanus.* Cell Tissue Res. **206**(3): 379–385. doi:10.1007/BF00237967. PMID:7388895.

Uni, Z., Platin, R., and Sklan, D. 1998. Cell proliferation in chicken intestinal epithelium occurs both in the crypt and along the villus. J. Comp. Physiol. B, **168**(4): 241–247. PMID: 9646500.

Waheed, A.A., and Gupta, P.D. 1997. Changes in structural and functional properties of rat intestinal brush border membrane during starvation. Life Sci. **61**(25): 2425–2433. doi:10.1016/S0024-3205(97)00977-6. PMID:9416761.

Willems, G. 1972. Cell renewal in the gastric mucosa. Digestion, **6**(1): 46–63. doi:10.1159/000197221. PMID:4260634.

Wilson, J.W., and Potten, C.S. 2004. Cell turnover: intestine and other tissues. *In* When cells die. Chapter 9. *Edited by* R.A. Lockshin and Z. Zakeri. John Wiley & Sons, Inc., New York. pp. 201–240.

Wurth, M.A., and Musacchia, X.J. 1964. Renewal of intestinal epithelium in the freshwater turtle, *Chrysemys picta*. Anat. Rec. **148**(3): 427–439. doi:10.1002/ar.1091480302. PMID:14153303.

Yamauchi, K., Kamisoyama, H., and Isshiki, Y. 1996. Effects of fasting and refeeding on structures of the intestinal villi and epithelial cells in White Leghorn hens. Br. Poult. Sci. **37**(5): 909–921. doi:10.1080/00071669608417922. PMID:9034581.